Visualization of Vacuolar Acidification-induced Transcription of Genes of Pathogens inside Macrophages□D

Natalia Martin-Orozco,*† Nicolas Touret,*† Michael L. Zaharik,‡§ Edwin Park,‖ Raoul Kopelman,‖ Samuel Miller,¶ B. Brett Finlay,‡ Philippe Gros,# and Sergio Grinstein*

*Cell Biology Program, Hospital for Sick Children and Department of Biochemistry, University of Toronto, Toronto, Ontario M5G 1X8, Canada; ‡Biotechnology Laboratory, University of British Columbia, Vancouver, British Columbia V6T1Z3, Canada; ‖Department of Chemistry, University of Michigan, Ann Arbor, MI 48109-1055; ¶Department of Microbiology and Laboratory of Medicine, University of Washington Medical School, Seattle, WA 98195; and #Department of Biochemistry, Center for the Study of Host Resistance, McGill University, Montreal, Quebec, Canada H3A 2T5

The objective of these studies was to analyze the role of the ionic environment of phagosomal vacuoles in the control of pathogens by macrophages. Digital imaging and flow cytometry were used to follow the induction of the *phoP* promoter of *Salmonella enterica* Typhimurium within live macrophages. Manipulating the Mg^{2+} concentration within the *Salmonella*-containing vacuole (SCV) was without effect on the early induction of PhoPQ. Moreover, direct measurement of $[Mg^{2+}]$ within the SCV using nanosensor particles showed that, during this initial period of *phoP* activation, the concentration of the divalent cation is rapidly regulated and stabilizes around 1 mM. Extrusion of other divalent cations via the Nramp1 efflux pump was similarly ruled out as an important contributor to the activation of the regulon. By contrast, induction of PhoP was greatly attenuated when the pH gradient across the SCV membrane was dissipated. A second, more modest pH-independent component of PhoP induction was unmasked by inhibition of the vacuolar proton pump. This second component was eliminated by pretreatment of cells with IFNγ, even though the cytokine augmented the overall PhoP response. These findings demonstrate the existence of at least three separate activators of *phoP* transcription: resting and IFNγ-stimulated pH-sensitive components, plus a pH-independent component.

INTRODUCTION

Salmonella species are responsible for several human diseases. *S. typhi* produces typhoid fever, an acute, life-threatening febrile illness, whereas *Salmonella* serovars Typhimurium and Enteritidis are a major cause of gastroenteritis (Mirza et al., 1996; House *et al.*, 2001; Young *et al.*, 2002). *Salmonella* has the ability to penetrate the gut epithelial barrier and can therefore cause systemic infection. Host resistance to systemic infection depends heavily on the ability of the innate immune system to control the proliferation and dissemination of *Salmonella*. Phagocytes of the lamina propria are a critical checkpoint in the prevention of systemic disease (Wick, 2004). They utilize a variety of mechanisms, including generation of reactive oxygen metabolites, proteases, and cationic peptides to eliminate invading mi-

croorganisms (Vazquez-Torres et al., 2000; Amer and Swanson, 2002; Rosenberger *et al.*, 2004). Limiting the availability of divalent metals by Nramp1-mediated efflux (natural resistance associated macrophage protein-1, Slc11a1) also contributes to bacterial elimination (Jabado *et al.*, 2004), in a manner that is incompletely understood. These and other components of the innate immune response are potentiated when the phagocytes are primed by IFNγ (Nauciel and Espinasse-Maes, 1992; Boehm *et al.*, 1997; Pie *et al.*, 1997; Mastroeni *et al.*, 1998; Monack *et al.*, 2004). Despite this abundance of cellular defenses, the bacteriostatic and bactericidal responses are sometimes insufficient to eliminate all bacteria, and *Salmonella* survive within the host leukocytes. In the latter case, infected macrophages and dendritic cells can reach the lymphatic system carrying viable bacteria to the spleen and liver (Vazquez-Torres *et al.*, 1999). Survival of *Salmonella* inside host cells involves at least two multifunctional virulence systems, the PhoPQ regulon and the *Salmonella* Pathogenicity Island 2 (SPI2; Miller *et al.*, 1989; Shea *et al.*, 1996). PhoPQ is a two-component regulatory system (PhoP and PhoQ) that is responsive to alterations in cation concentration (Groisman *et al.*, 1997) and is essential for intracellular survival of *Salmonella*. It acts, at least in part, by enhancing resistance to macrophage defenses, including antimicrobial peptides (Guo *et al.*, 1997, 1998; Guina *et al.*, 2000). Importantly, PhoPQ is also required in the first hours of invasion to prevent fusion of the *Salmonella*-containing

□D The online version of this article contains supplemental material at *MBC Online* (http://www.molbiolcell.org).

† These authors contributed equally to this work.

§ Present address: UBC CDC, 655 West 12th Avenue, Vancouver, British Columbia V5Z4R4, Canada.

Address correspondence to: Sergio Grinstein (sga@sickkids.ca).

vacuoles (SCV) with host cell lysosomes (Garvis *et al.*, 2001), thereby minimizing the delivery of microbicidal enzymes.

The mechanism of intracellular activation of these bacterial virulence genes is poorly understood. In vitro experiments where the composition of the liquid culture medium was modified provided direct evidence that PhoPQ is activated when the concentration of Mg^{2+} is reduced (Garcia Vescovi *et al.*, 1996). It has therefore been concluded that PhoPQ-regulated genes, which include PhoP itself (Soncini *et al.*, 1995), are induced in response to Mg^{2+} starvation within the SCV. However, other factors have also been identified to activate the PhoPQ complex in vitro, including acidification (Bearson *et al.*, 1998) and cationic peptides (Bader *et al.*, 2003; Bader *et al.*, 2005). Despite the wealth of knowledge of potential regulatory factors, the determinants of PhoPQ activation within the SCV in infected cells at early times of invasion remain obscure. This can be attributed largely to the difficulty of assessing bacterial gene expression while *Salmonella* reside within mammalian host cells and to the asynchronous nature of the infection and gene induction events in populations of cells exposed to multiple bacteria. In this study, we overcame these difficulties by directly monitoring *phoP* promoter induction in individual cells by means of fluorescence. To measure the activity of *phoP*, we generated a bacterial expression vector encoding the green fluorescent protein (GFP) under the control of the *phoP* promoter. An unstable, short-lived variant of GFP was used to reduce hysteresis and thereby improved the temporal resolution of the measurements. The vector was introduced into *S. enterica* Typhimurium 14028, which were used to infect either primary or cultured murine macrophages. Detailed analysis and validation of the system was initially performed by microscopy, while statistically robust data were obtained by analyzing large numbers of cells by flow cytometry. Using this system, we were able to establish the precise kinetics of PhoP induction and to evaluate the contribution of Mg^{2+}, H^+ and Nramp1 to the response. In addition, we analyzed the effect of pretreatment of the macrophages with IFNγ on bacterial gene induction. Together, our results demonstrate that acidification of the phagosome lumen is the major factor leading to the induction of the *phoP* promoter in intracellular *Salmonella*.

MATERIALS AND METHODS

Construction of a destabilized *phoP*::GFP fusion. The *lac* promoter from pGFPmut3.1 (LVA; Clontech, Palo Alto, CA) was deleted by a *Sal*I-*Sap*I sequential digest, followed by repairing the recessed ends with the Klenow fragment of *Escherichia coli* DNA polymerase and blunt-end ligation using T4 DNA ligase. A fragment containing the *phoP* regulatory region and extending into the *phoP* coding region was amplified by PCR from *Salmonella* Typhimurium 14028s genomic DNA using the oligonucleotides phoPQE1 (5′-TCGAC-GAATTCTTAAATAATGCCTGCC-3′) and phoRPH3 (5′-ATGTGGAAT-GAAGCTTCGTCACGTAGTC-3′). This fragment was ligated into the cloning vector pCR2.1 (Invitrogen, Carlsbad, CA) and a *Xba*I-*Kpn*I fragment ligated into similarly digested *lac*⁻ pGFPmut3.1 to yield a 1.5-kbp *phoP*::GFP fusion cassette. This cassette was isolated as an *Apa*I-*Xba*I fragment and cloned into the low copy-number vector pACYC184 (NEB, Ipswich, MA) digested with *Eco*RV to yield pMLZ205.

Bacterial Strains and Culture Conditions

Salmonella Typhimurium 14028, wild type, and *Salmonella* Typhimurium 14028 CS009 *phoQ101*:: MudJ (Miller *et al.,* 1989) were transformed with *phoP*::GFP expression vector pMLZ205. These bacteria were grown in Luria broth (Difco, Detroit, MI) supplemented with 2.5 μg/ml chloramphenicol and 10 mM $MgCl_2$ for 12 h at 37°C. A 1:30 dilution of this culture was grown until optical density reached 0.5 at 600 nm, which corresponded to 2×10^8 cells/ml.

For in vitro induction of *phoP*::GFP, *Salmonella* Typhimurium strains were grown in minimum medium M9 (0.25 M Na_2HPO_4, 0.11 M KH_2PO_4, 0.0438 M NaCl, 0.094 M NH_4Cl, 20 mM glucose; Sigma-Aldrich, St. Louis, MO) sup-

plemented with the indicated $MgCl_2$ concentration and adjusted to the indicated pH. After 4 h of culture at 37°C, bacteria were harvested, washed extensively with phosphate-buffered saline (PBS), and fixed for 1 h with 4% paraformaldehyde in PBS solution. Finally, samples of bacterial suspension were washed with PBS supplemented with 0.5% BSA and 0.1% azide before flow cytometric analysis. To monitor the kinetics of induction of *phoP*::GFP in vitro, bacteria were grown in 2 ml of minimal medium containing 0.01 mM $MgCl_2$, pH 6, to an optical density of 0.5. A 150-μl aliquot of the culture was then added to 1 ml of PBS at times ranging from 0 to 180 min for determination of GFP fluorescence intensity using a Hitachi spectrofluorimeter with excitation at 490 nm and emission at 520 nm, whereas in parallel monitoring the optical density at 600 nm using a Bio-Rad spectrophotometer (Richmond, CA). In experiments where intravacuolar Mg^{2+} was analyzed, the bacteria were labeled with 28.6 μM DAPI (Molecular Probes, Eugene, OR) in PBS for 20 min at 37°C for detection by fluorescence microscopy.

Mice

129Sv wild-type mice and their Nramp1-deficient counterparts were maintained as a breeding colony at McGill University (Montreal, Canada). Mice were inoculated with 3% sodium thioglycolate in the peritoneal cavity and cell exudates were harvested at day 4 by washing the peritoneum with 10 ml of PBS. Pooled cells from groups of five mice were plated on glass coverslips placed at the bottom of six-well plates and overlaid with DMEM with 10% fetal calf serum (FCS), followed by incubation for at least 3 h at 37°C. Nonadherent cells were washed and macrophages were infected as described below.

Infection of Macrophages with **Salmonella** Typhimurium

RAW264.7 macrophages (TIB-71) were purchased from ATCC (Rockville, MD) and were grown in antibiotic-free DMEM supplemented with 10% FCS and 2 mM L-glutamine. The night before the experiment, 10^6 RAW264.7 cells were seeded onto 25-mm glass coverslips. Infections with *Salmonella* Typhimurium pMLZ205 were done at a multiplicity of infection (MOI) of 10. After 15 min of invasion at 37°C, cells were washed three times with DMEM followed by the addition of 50 μg/ml gentamicin and further incubation at 37°C for the specified time. For activation, RAW 264.7 cells were cultured with 100 U/ml recombinant murine IFNγ (Peprotech Canada, Ottawa, Canada) for 18 h at 37°C. Blockage of the vacuolar proton pump (V-ATPase) was obtained with 30 nM of concanamycin A (Kamiya Biomedical Company, Thousand Oaks, CA). To introduce Mg^{2+} into SCV, cells were treated with 4 μM A23187 or 1 μM ionomycin in medium devoid of Ca^{2+} and containing 10 mM $MgCl_2$.

Detection of **Salmonella** Typhimurium in Infected RAW264.7 Macrophages

Extracellular *Salmonella* Typhimurium adherent to infected RAW264.7 cells were detected by immunostaining before permeabilization. To minimize spurious binding of antibodies to Fc receptors, the latter were blocked by pretreatment with 0.5 μg/ml rat anti-mouse CD16/CD32 (BD Biosciences, San Diego, CA) for 30 min at 4°C. This was followed by the addition of anti-*Salmonella* mouse monoclonal antibody (MAB746; Chemicon International, Temecula, CA) for 20 min at 4°C. The cells were then washed with 0.5% BSA-supplemented PBS and stained with Alexa 633-conjugated rat anti-mouse (Molecular Probes). For detection of total (extracellular plus intracellular) *Salmonella* the cells were fixed with 4% paraformaldehyde for 20 min and permeabilized with PBS containing 1% saponin, 0.5% BSA followed by the addition of rabbit anti-*Salmonella* antibodies (Difco, Becton Dickinson, Detroit, MI). Cy3-conjugated goat anti-rabbit (Jackson ImmunoResearch Laboratories, West Grove, PA) was used as secondary label. Cells were visualized with a Leica IRE DR2 microscope (Deerfield, IL) using a 100× oil immersion objective and digital images were acquired using an Orca II ER camera (Hamamatsu Photonics, Bridgewater, NJ) driven by the Openlab 3 software (Improvision, Lexington, MA).

Flow Cytometry

RAW264.7 cells were detached from coverslips with 0.25% trypsin and 1 mM EDTA and fixed with 2% paraformaldehyde for 20 min. Intracellular staining was performed as described above, except that Alexa633-conjugated goat anti-rabbit (Molecular Probes) or Cy5-conjugated donkey anti-rabbit (Jackson ImmunoResearch Laboratories) were used as secondary antibodies. A minimum of 10^4 macrophages was analyzed for each condition in a FACS-Calibur cytometer (Becton-Dickinson, San Jose, CA). Live macrophages, which constituted ≥90% of the population of cells, were identified based on their characteristic forward and side scattering properties. Subsequent analysis of the resulting files was performed with Flow Jo software (Tree Star Flow Jo, San Carlos, CA). Sequential gating of live macrophages (based on forward and side scatter patterns), infected (LPS positive-FL-4) and *phoP*-induced (GFP positive) cells was done to calculate the percentage of infected macrophages and measure the fluorescence intensity of GFP. For detection of the in vitro induction of *phoP*-GFP in *Salmonella*, 10^5 bacteria were analyzed by flow cytometry per condition. Expression of Nramp1 in transfected RAW264.7 cells

(Govoni *et al.,* 1999) was verified by immunostaining the myc epitope in permeabilized cells, followed by flow cytometric analysis.

Quantification of Live Bacteria

After infection for the indicated times, RAW264.7 macrophages were washed four times with 3 ml of PBS and lysed with 1% saponin in PBS. Serial dilutions of the lysate were plated in LB-agar containing 30 μg/ml chloramphenicol. Plates were cultured for 18 h at 37°C and bacterial colonies were counted. A similar plating protocol was applied to bacteria that were prelabeled with DAPI. Under the conditions used, the nucleic acid stain had no effect on bacterial viability.

Measurements of the pH of SCV

Salmonella Typhimurium 14028 were labeled with fluorescein isothiocyanate as in (Cuellar-Mata *et al.,* 2002) and used to infect RAW264.7 macrophages, as described above. The infected macrophages were placed in a Leiden chamber kept at 37°C and bathed with buffer A (140 mM NaCl, 5 mM KCl, 10 mM glucose, 1 mM MgCl$_2$, 10 mM HEPES, pH 7.4). For pH measurements the chamber was mounted on a Leica DMIRB inverted microscope equipped for digital ratio imaging as detailed in (Cuellar-Mata *et al.,* 2002). The pH was estimated from the ratio of fluorescence emission using 490 $\pm$ 10 nm and 440 $\pm$ 10 nm excitation and calibrated in situ.

Measurement of [Mg^{2+}] in the SCV using PEBBLE Nanotechnology

To selectively detect [Mg^{2+}] within the lumen of the SCV, we used the coumarin 343 (C343) and Texas Red (TxRed)-loaded nanosensor called PEBBLE (probe encapsulated by biologically localized embedding). This detection system, described in detail in (Park *et al.,* 2003), allows fluorometric quantitation of [Mg^{2+}] in a manner that is independent of the concentration of the probe and is minimally affected by alterations in focal plane. Because the pH and calcium concentration inside the vacuole are unknown and may vary during the course of the experiments, it was important to ensure that the probe would be minimally affected by these parameters. To test the effects of [Ca^{2+}] and pH on the responsiveness of C343 to [Mg^{2+}], we measured the fluorescence emission of a solution of the probe (15 μM in 100 mM MOPS and 200 μM of EDTA, pH 7) at 495 $\pm$ 2.5 nm, with excitation at 445 $\pm$ 2.5 nm, using a Hitachi spectrofluorimeter (Pleasanton, CA). The emission changes induced by varying [Mg^{2+}] were monitored at different pH levels and in the presence and absence of 2 mM CaCl$_2$. Data transfer and analysis were performed with Microsoft Excel (Redmond, WA) and Graphpad Prism 4.0 (Sorrento, CA), respectively. As illustrated in Supplementary Figure 1A, neither the apparent K$_d$ for Mg^{2+} nor the maximal fluorescence change induced by this cation were significantly affected by addition of 2 mM calcium, in agreement with the earlier findings of (Park *et al.,* 2003). Similarly, alterations in pH over 1.5 U, encompassing the range of values found during the course of vacuolar maturation, had only small effects on the Mg^{2+} responsiveness of the dye. The K$_d$ changed very modestly (17%) over this pH range (Supplementary Figure 1B).

To measure [Mg^{2+}] in the vacuoles, a suspension of 10 mg/ml C343/TxRed PEBBLEs was sonicated for 20 min and centrifuged at 1300 rpm for 10 min to remove aggregates, before addition to the RAW264.7 macrophages. In parallel, a suspension of *Salmonella* Typhimurium 14028 was prelabeled with 28.6 μM DAPI (Molecular Probes) for 20 min at 37°C. After extensive washes with PBS the labeled bacteria and the PEBBLE suspension were added together to macrophages bathed in buffer A containing 100 μM EDTA and the indicated concentrations of MgCl$_2$. Cells were placed in a Leiden chamber kept at 37°C, and overlaid with buffer A. The chamber was mounted on a Leica DMIRB inverted microscope equipped with suitable filters and dichroic mirrors. [Mg^{2+}] was estimated from the ratio of fluorescence emission at 460–640 nm while exciting the sample at 445 nm. Calibration was performed ex vivo using dilutions of PEBBLEs in buffer A containing varying concentrations of MgCl$_2$. Imaging of the nanoparticles in vacuoles containing bacteria was performed on a spinning-disk confocal microscope. For these experiments RAW264.7 cells were cultured for 5 min at 37°C with 10 mg/ml C343/TxRed PEBBLEs and infected simultaneously with a *Salmonella* strain that expresses GFP constitutively. To test the Mg^{2+} responsiveness of the PEBBLEs, regions of interest were defined that encompassed labeled vacuoles, and fluorescence intensities were acquired before and after addition of 10 mM MgCl$_2$ plus 1 μM ionomycin, with or without 10 mM NH$_4$Cl or 30 nM concanamycin A (CcA).

RESULTS

Validation of the phoP::GFP Expression System as a Measure of PhoP Activation in Salmonella Typhimurium

We constructed a plasmid encoding GFP under the control of the *phoP* promoter (*phoP*::GFP) to study the intracellular signals that induce *phoP* expression within macrophages. To

minimize hysteresis and thereby improve the temporal resolution of the determinations we used a variant of GFP with a much-reduced half-life ($\approx$40 min in *E. coli*). The destabilization of GFP is the result of mutations in its C-terminal tail that target the protein for degradation by bacterial proteases.

Salmonella Typhimurium were transformed with the plasmid encoding *phoP*::GFP and incubated under conditions known to induce the expression of PhoPQ-regulated genes, to verify the usefulness of the plasmid as an index of PhoPQ activation. Figure 1A shows FACS profiles of GFP expression by *Salmonella* Typhimurium suspensions incubated in media of varying pH and Mg^{2+} concentration. GFP expression was insignificant at all pH values tested when [Mg^{2+}] = 10 mM. Expression was also marginal when [Mg^{2+}] and pH approximated the levels that prevail in mammalian serum, namely near-neutral pH and $\approx$1 mM Mg^{2+}. However, as anticipated from published measurements of PhoPQ activation (Garcia Vescovi *et al.,* 1996), *phoP*::GFP expression became detectable at submillimolar [Mg^{2+}]. Of note, the modest expression noted at neutral pH when [Mg^{2+}] was reduced below 1 mM was greatly magnified when the medium was acidified (gray and black histograms in Figure 1). In fact, acidification induced a sizable induction of GFP at 1 mM Mg^{2+} and amplified the effect of Mg^{2+} depletion even at the lowest concentrations of Mg^{2+} tested. These results demonstrate that our expression construct of *phoP*::GFP is responsive to both reduced Mg^{2+} and acidic pH. Quantitative estimates of the total bacterial fluorescence (TF) under each condition, calculated as the product of the mean fluorescence intensity of the bacteria that expressed GFP times the percentage of fluorescent bacteria, are summarized in Figure 1B. Note that the viability of the bacteria was compromised when incubated at pH 5 and [Mg^{2+}] < 1 mM. The kinetics of expression of GFP under conditions of optimal induction (0.01 mM Mg^{2+}, pH 6.0) are illustrated in Figure 1C. GFP accumulation is detectable after $\geq$1 h and increases markedly for at least 2 additional hours.

To ensure that, as in the native system, *phoP* is autoregulated by PhoPQ, we utilized *phoQ*-deficient bacteria (Soncini *et al.,* 1995). *Salmonella* Typhimurium 14028 CS009 *phoQ101*::Mu*d*J were transformed with the pMLZ205 plasmid encoding *phoP*::GFP and subjected to the same incubation conditions described for wild-type bacteria. As illustrated in Figure 1A neither reduced pH nor omission of Mg^{2+} induced GFP expression in these bacteria, confirming the dependence on PhoQ. Because PhoP protein expression is itself dependent on PhoQ (Soncini *et al.,* 1995; Groisman, 2001), our data cannot resolve whether one or both of these proteins are required for the activation. In any event, these results imply that *phoP*::GFP is a suitable and sensitive probe for the spectroscopic assessment of PhoPQ activity in live bacteria.

Monitoring phoP::GFP during Salmonella Typhimurium Invasion of Macrophages

To define the factors that activate PhoPQ within the SCV, RAW264.7 macrophages were infected with *Salmonella* Typhimurium transformed with *phoP*::GFP. Immunostaining of the bacteria before and after permeabilization determined whether they had entered the cell or were merely adherent to its surface. One of the few cells found to retain external adherent bacteria after washing is shown in Figure 2, A–D, to illustrate the method. Adherent extracellular bacteria invariably failed to express GFP, consistent with the pH (7.4) and [Mg^{2+}] (1 mM) of the medium used to incubate mammalian cells. By contrast, most of the intracellular bacteria accumulated GFP within 1 h of infection.
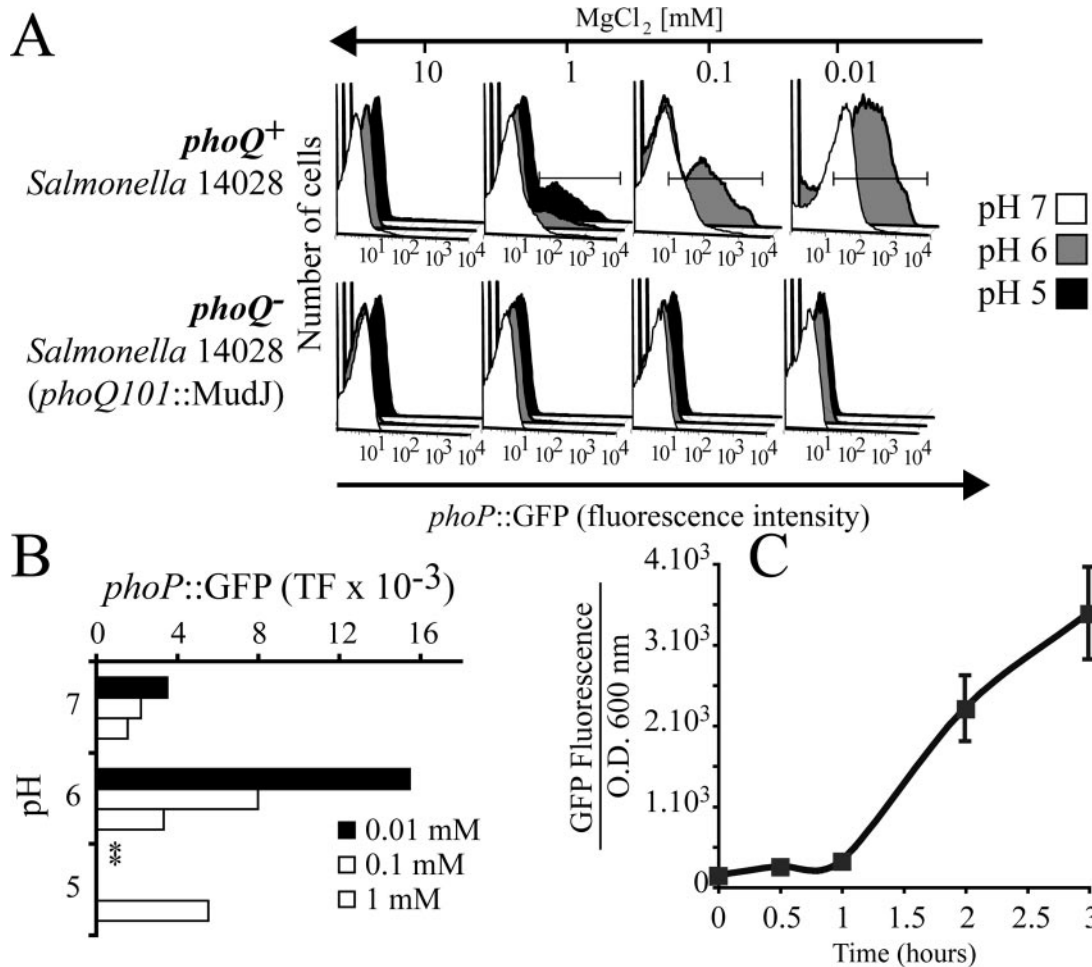
Figure 1. Expression of *phoP*::GFP by *Salmonella* Typhimurium in media of varying [Mg^{2+}] and pH. *Salmonella* Typhimurium 14028 *phoQ$^+$* and the mutant *phoQ101::MudJ phoQ$^-$* were transformed with the plasmid pMLZ205 that encodes *phoP*::GFP. A small inoculum was grown in medium M9 supplemented with the indicated MgCl$_2$ concentration and adjusted to the specified pH. After 5 h of culture, the bacteria were harvested and fluorescence was analyzed by flow cytometry. (A) Representative histograms of one experiment; (B) quantitation of total fluorescence from histograms like those shown in A (TF, mean fluorescence multiplied by the % of GFP-positive bacteria). Where indicated by asterisks, bacterial viability was compromised and fluorescence was not quantified. Similar results were obtained in three independent experiments. (C) Time course of GFP expression in *phoP*::GFP *Salmonella* suspended in M9 minimal medium with 0.01 mM MgCl$_2$ at pH 6.0. Aliquots of the suspension were withdrawn at the indicated times and GFP fluorescence and optical density at 600 nm were measured as described in *Materials and Methods.* Data are representative of three similar experiments.

The expression of *phoP*::GFP in *Salmonella*-infected macrophages could be easily recorded by confocal microscopy (Supplementary Figure 2). In fact, the large differential between the uninduced and induced bacteria was so great that it exceeded the dynamic range of our CCD detector. For this reason, we chose to systematically analyze the rate and extent of *phoP*::GFP induction using flow cytometry. Intact macrophages, defined by their side and forward scattering features, were gated to analyze the fluorescence emitted by anti-LPS (ordinate in Figure 2E) and GFP (abscissa in Figure 2E). The anti-LPS signal provided an estimate of the number of bacteria per infected cell, whereas GFP fluorescence intensity reflected the activity of the *phoP* promoter. Microscopic analysis, as well as anti-LPS staining before and after permeabilization of the infected macrophages, revealed that the fraction of extracellular adherent bacteria was negligible after the cells were treated with trypsin-EDTA for detachment (unpublished data). More importantly, although GFP fluorescence was insignificant immediately after the 15-min invasion period (time 0 in Figure 2E), more than 50% of the

infected macrophages contained *Salmonella* Typhimurium expressing *phoP*::GFP 30 min after invasion (Figure 2E, 0.5 h, and Figure 3B). The induction of *phoP*::GFP increased markedly in most of the infected macrophages for at least 3 h (Figures 2E and 3C). This is likely due to additional activation of *phoP*, but also to accumulation of the fluorescent protein product over time, which would occur even if the promoter activity remained constant.

To facilitate comparison between conditions and among experiments, we normalized the total fluorescence of *phoP*::GFP from the cytometric profiles of infected macrophages, like that in Figure 3A. TF was defined as the product of the fraction of infected macrophages (Figure 3B) times the mean fluorescence of individual infected macrophages (Figure 3C). As illustrated in Figure 3E, the vast majority of macrophages were infected under the conditions used and the fraction of infected cells remained constant throughout the period analyzed. Moreover, the number of intracellular bacteria increased only marginally during the first 3 h after invasion (Figure 3F). To validate that LPS staining was a
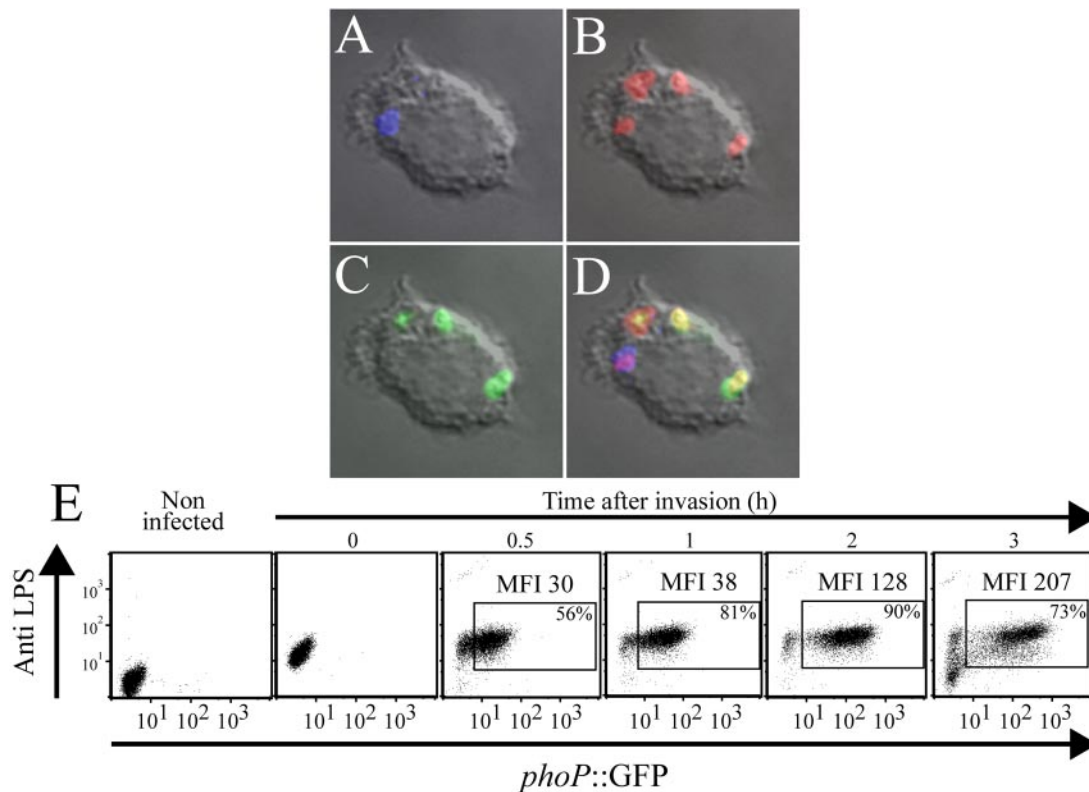
Figure 2. Expression of *phoP*::GFP by *Salmonella* Typhimurium inside macrophages. (A–D) RAW264.7 macrophages were infected with *Salmonella* Typhimurium-pMLZ205 at a MOI of 10. After 60 min, the cells were fixed and extracellular bacteria were identified by labeling with anti-LPS antibodies, followed by fluorescent secondary antibody (blue in A and D). Presence of extracellular bacteria after 60 min is extremely rare, but one such case is shown here to illustrate that external bacteria do not express GFP. The cells were next permeabilized and total bacteria were labeled with primary and secondary antibodies, as above (red in B and D). The fluorescence of GFP was directly visualized (green in C and D). (E) RAW264.7 macrophages were infected with *Salmonella* Typhimurium-pMLZ205 for 15 min at a MOI of 10, followed by removal of extracellular bacteria and addition of 5 μM gentamicin. After the indicated periods, the cells were fixed, permeabilized, and stained with anti-LPS and secondary antibody as above. Cells were analyzed by flow cytometry, gating on the population of live macrophages (90%) based on their characteristic forward and side scattering properties. Dot plots (scattergrams) show the number of cell-associated bacteria (identified by anti-LPS; ordinate) versus the expression of GFP (abscissa) as a function of time after infection. The values in the insets indicate the percentage of infected macrophages where *phoP*::GFP is induced. Data are representative of eight similar experiments. MFI, mean fluorescence intensity of GFP in the gated population.

suitable indicator of intracellular bacterial number, we verified bacterial numbers by lysing the cells with detergent at varying times, plating the extracted bacteria, and counting the emerging colonies (Figure 3G). No variation of the initial number of ingested bacteria was observed after 3 h after infection. Despite the constancy of the bacterial load, there was a small (7% average in 8 experiments) reduction between 2 and 3 h in the fraction of cells containing *phoP*::GFP-expressing bacteria (Figure 3B). In fact, the reappearance of LPS-negative macrophages at later times in Figure 2 suggests that bacteria were killed in a subpopulation of cells. In this case, the total number of bacteria may have remained approximately constant only if some bacterial replication occurred in the remaining infected cells. Together, these data indicate that PhoPQ is activated rapidly in bacteria within SCV and that induction of the *PhoP* precedes bacterial multiplication, in agreement with earlier findings (Alpuche Aranda *et al.,* 1992). The faster induction of *phoP* in vivo than found in vitro suggests that factors other than pH and Mg^{2+} contribute to activation of the promoter in the vacuole. In this regard, Bader *et al.* (2005) very recently reported that *phoP* is sensitive also to antimicrobial peptides synthesized and delivered to the vacuole by host cells. In

summary, it appears that expression of GFP in bacteria transformed with *phoP*::GFP is a sensitive tool to assess the determinants of PhoPQ activation in macrophages.

Early Activation of PhoP Is Not Modified by Variation of Extracellular [Mg^{2+}]

A considerable amount of information generated largely by Groisman and colleagues (Garcia Vescovi *et al.,* 1996) indicates that PhoPQ is highly sensitive to alterations in the concentration of Mg^{2+}. To estimate the contribution of [Mg^{2+}] as a modulator of PhoPQ induction within the SVC, we varied the concentration of Mg^{2+} in the medium that is trapped within the forming vacuole. The rationale of this experiment was that reduction of luminal [Mg^{2+}] to the threshold level where PhoPQ is activated would be reached later if a larger amount of the cation needs to be extruded from the vacuole. [Mg^{2+}] in the medium was varied over greater than one order of magnitude (from 0.5 to 10 mM) and expression of GFP in infected macrophages was analyzed as in Figures 2 and 3. As anticipated, the mean fluorescence intensity of the macrophage population was somewhat greater in cells incubated at subphysiological (0.5 mM) [Mg^{2+}] (Figure 4A). Under these conditions, expression of
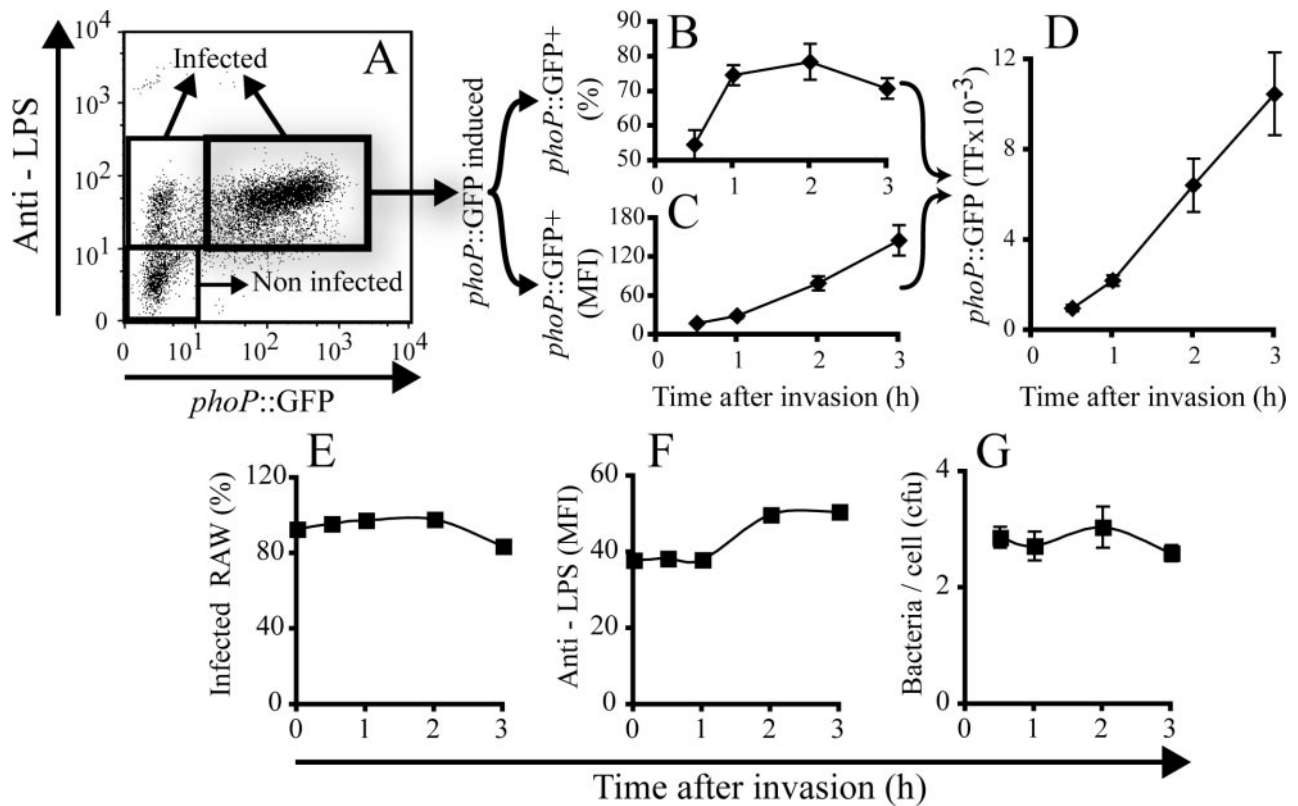
Figure 3. Analysis of *phoP*::GFP expression in *Salmonella*-infected RAW264.7 macrophages. (A) Definition of the different subpopulations of cells in a typical dot plot. Noninfected cells have LPS staining indistinguishable from untreated cells, whereas infected cells have significantly higher levels of LPS signal. Infected cells were subdivided into those that had negligible *phoP*::GFP induction (insignificant green fluorescence) and those with distinct induction. (B) Fraction of cells expressing *phoP*::GFP as a function of time after invasion; (C) mean fluorescence intensity (MFI) of the subpopulation of *phoP*::GFP expressing cells as a function of time. (D) Total fluorescence (TF), calculated as the product of the MFI times the fraction of cells expressing *phoP*::GFP. (E) Fraction of infected cells. (F) Quantitation of LPS staining, a measure of bacterial number. (G) Quantitation of viable bacteria recovered from infected cultures, performed by cell lysis and plating of lysates on LB agar plates. Data in B–D are a compilation of eight independent experiments, and E, F, and G is one representative experiment of eight experiments with similar results.

GFP may be initiated by exposure to the culture medium even before the bacteria enter the cells (see Figure 1). High [Mg^{2+}] slightly depressed the extent of total GFP expression, compared with the physiological concentration (Figure 4A). On closer inspection of the data it became apparent that high [Mg^{2+}] reduced the ability of *Salmonella* to invade the mac-
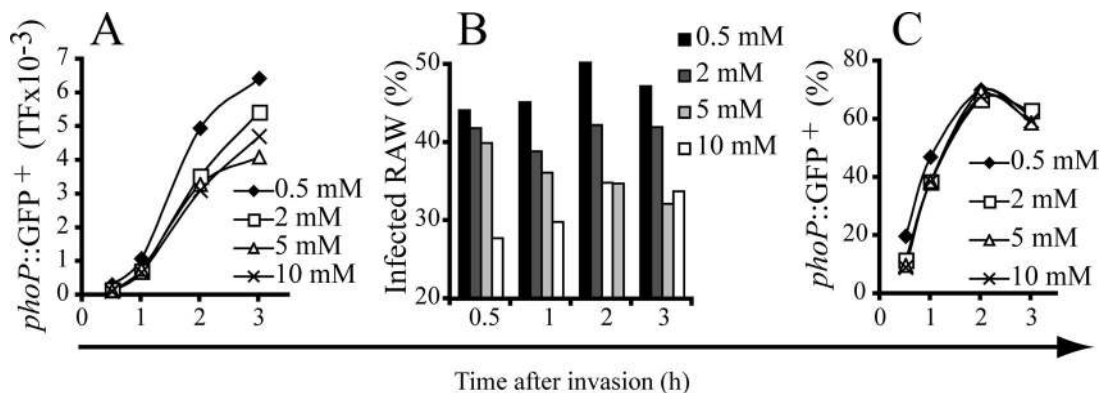

Figure 4. Assessment of the role of [Mg^{2+}] in PhoPQ induction. (A–C) RAW264.7 macrophages were bathed in medium containing the indicated [Mg^{2+}] and were infected with *Salmonella* Typhimurium-pMLZ205 at a MOI of 10 for 15 min. Extracellular bacteria were washed and the infected cells were incubated for the indicated times. The total GFP fluorescence (TF), calculated as in Figure 2 is shown in A, whereas the fraction of infected cells is presented in B and the proportion of macrophages where *phoP*::GFP is induced is shown in C. Data are representative of five experiments with similar results.
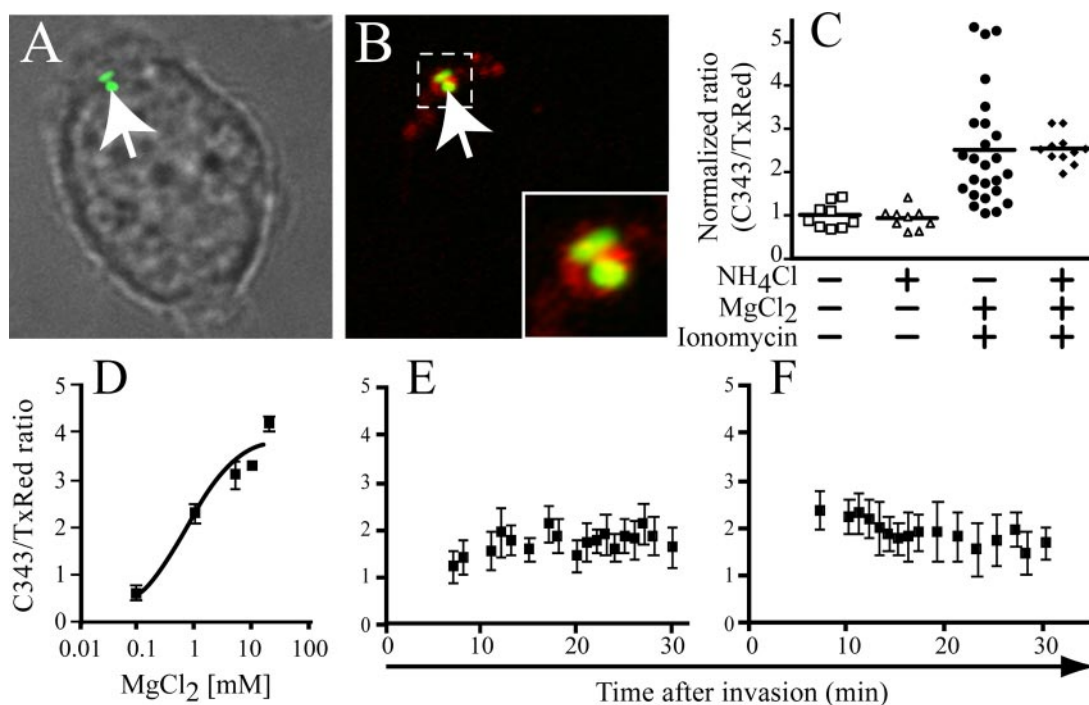
Figure 5. Measurements of [Mg^{2+}] in SCV using PEBBLEs. (A and B) Imaging of RAW264.7 macrophages incubated for 5 min with PEBBLEs and a *Salmonella* strain that expresses GFP constitutively. After washing, DIC and confocal fluorescence images were acquired. (A) An overlay of the DIC and green fluorescence images, illustrating the location of bacteria (arrow) within an infected cell. (B) An overlay of the green (bacterial) and red (TxRed in PEBBLEs) fluorescence. The area denoted by the dotted line is enlarged in the inset. (C) RAW264.7 macrophages were loaded with PEBBLEs and the fluorescence of C343 and TxRed was determined by digital imaging under various conditions. Cells were initially bathed in a NaCl buffer deprived of Mg^{2+} (leftmost column). The cells were then treated with either 10 mM NH$_4$Cl, a combination of 10 mM MgCl$_2$ and 1 μM ionomycin, or all three agents, as indicated. Data from three experiments are illustrated. The ratio of C343 to TxRed was normalized to facilitate comparison between experiments. (D) In vitro calibration of PEBBLEs. The fluorescence ratio of the C343 and TxRed signals (ordinate) is presented as a function of [Mg^{2+}] (abscissa). (E and F) Determination of free [Mg^{2+}] in the SCV. SCV were loaded with PEBBLEs during infection and their fluorescence ratio was monitored over time by digital imaging, while identifying the location of the bacteria by their DAPI fluorescence (see *Materials and Methods*). The [Mg^{2+}] of the medium in E and F was 0.5 mM and 2 mM, respectively. Data in E and F are means $\pm$ SE of 10 determinations for each time point, obtained from four independent experiments.

rophages (Figure 4B), but not the extent of GFP expression in the fraction of cells that were infected (Figure 4C). The kinetics of expression in the infected cells was similarly unaltered. These experiments highlight the advantages of cytometric analysis of single cells, because the difference in global GFP accumulation of the cellular population could be misinterpreted as a reduced expression of PhoP per bacterium. Instead, high [Mg^{2+}] depressed fluorescence accumulation by reducing bacterial invasiveness, without alteration in the ability of internalized bacteria to induce PhoP.

Direct Measurements of the Luminal [Mg^{2+}] of SCV

The preceding experiments were intended to manipulate luminal [Mg^{2+}] after invasion, but the effectiveness of these maneuvers was not verified directly. As an alternative and more direct approach, we implemented a novel method for the measurement of [Mg^{2+}] inside SCV in live macrophages. The method is based on the manufacture and delivery of ion-selective nanosensors called PEBBLEs. The operating principles and synthesis of PEBBLEs are described in Clark *et al.* (1999) and Park *et al.* (2003). Briefly, these nanoparticles (average diameter $\approx$ 20 nm) consist of a polyacrylamide matrix wherein ion-sensitive fluorophores and reference dyes are trapped. For Mg^{2+} determinations, coumarin 343 (C343) is used as the ion-selective probe, and TxRed is added as a Mg^{2+}-insensitive reference, intended to correct for vari-

ations in focal plane and/or sensitivity of the optical hardware during the course of the measurements. The cross-linking of the polyacrylamide matrix of the PEBBLEs is designed to retain the fluorophores, while allowing permeation of inorganic ions, including Mg^{2+}. The size of the particles themselves is sufficiently small to allow uptake by cells via endocytosis or pinocytosis (Park *et al.*, 2003).

The responsiveness of the coumarin PEBBLEs to [Mg^{2+}], in vitro and in situ, is illustrated in Figure 5, C and D. In vitro determination of the ratio of the emission of C343 to that of TxRed is plotted as a function of the concentration of the cation in Figure 5D, which shows that the probes have an adequate dynamic range between 0.1 and 10 mM [Mg^{2+}]. Of note, preliminary experiments confirmed that C343 is virtually insensitive to calcium in the physiological range, i.e., between 0 and 2 mM (Supplementary Figure 1A), and is only modestly affected by pH in the 5.5–7.0 range expected to exist in the vacuoles (Supplementary Figure 1B).

To carry out quantitative ratiometric measurements of PEBBLE fluorescence in bacterial vacuoles, *Salmonella* were prestained with DAPI and the cells were visualized with UV light to verify the location of the SCV. Independent experiments were performed to ascertain that DAPI staining was without effect on the viability of the bacteria, as determined by plating and counting colonies (see *Materials and Methods*). In Figure 5, A–C, RAW264.7 macrophages were loaded with

Table 1. Direct measurement of $[Mg^{2+}]$ in vacuoles loaded with PEBBLEs

Loading concentration of MgCl$_2$ (mM)	Nontreated		CcA-treated	
	Basal	10 mM MgCl$_2$ + ionophore	Basal	10 mM MgCl$_2$ + ionophore
0	1.35 ± 0.07	2.28 ± 0.08	1.31 ± 0.06	2.75 ± 0.11
5	1.37 ± 0.09	2.12 ± 0.16	1.40 ± 0.12	2.27 ± 0.21
10	2.48 ± 0.07	2.94 ± 0.11	2.12 ± 0.24	3.06 ± 0.26

RAW macrophages were loaded for 10 min with PEBBLEs (10 mg/ml) in a Ca^{2+}-free NaCl solution containing the indicated amount of MgCl$_2$ in the presence or absence of 30 nM concanamycin A (CcA). After acquisition of C343 and TxRed fluorescent signal at the basal level, cells were treated with 1 μM of ionomycin in the presence of 10 mM MgCl$_2$. Data are expressed as the mean ratio of C343/TxRed signals $\pm$ SE of three independent experiments.

the nanoparticles and fluorescence intensity was recorded in the organelles labeled with the PEBBLEs that contained also bacteria. A sizable increase in the ratio of C343/TxRed was detected when 10 mM MgCl$_2$ was added together with 1 μM ionomycin, allowing the cations to rapidly enter and distribute throughout the cells, including the lumen of the vacuoles (Figure 5C and Table 1). The sensitivity of the C343/TxRed PEBBLEs toward Mg^{2+} was not affected by relieving the vacuolar acidification through the addition of NH$_4$Cl, reinforcing the observation that the probe is largely unaffected by pH in the range studied (Supplementary Figure 1B).

The experiments in Figure 4A were made under the assumption that changing extracellular [MgCl$_2$] would result in a parallel change in vacuolar [MgCl$_2$]. The availability of PEBBLEs enabled us to test this presumption. The results of vacuolar $[Mg^{2+}]$ measurements after uptake in media of varying composition are summarized in Table 1. Of note, the fluorescence ratio of the PEBBLEs was not significantly different when 0 or 5 mM MgCl$_2$ was present during sealing, and vacuolar $[Mg^{2+}]$ was higher only when 10 mM was used. These findings suggest that in cells bathed at or near the physiological extracellular [MgCl$_2$] ($\approx$2 mM) the vacuolar $[Mg^{2+}]$ is maintained, possibly regulated near 1 mM (the concentration calculated from the PEBBLE fluorescence ratio) and that regulation can be overcome only when considerably greater (10 mM) concentrations are present at the time of sealing.

A more detailed analysis of the changes of vacuolar $[Mg^{2+}]$ over time was performed next. At the earliest time that we were able to measure (5–10 min after invasion), the luminal concentration of Mg^{2+}, deduced from the fluorescence ratio, was similar to the extracellular concentration (0.5 mM in Figure 5E and 2 mM in 5F). More importantly, the measured concentration appeared to drift gradually during the course of the next 20–25 min toward a concentration of 1 mM, regardless of the initial concentration, consistent with the results in Table 1 and with the interpretation that vacuolar $[Mg^{2+}]$ is regulated. Because $[Mg^{2+}]$ had equilibrated after 30 min, a time when expression of *phoP*::GFP by bacteria infecting macrophages was unambiguous, we concluded that a decreased concentration of the divalent cation (below 1 mM) is not the primary cause of PhoP induced transcription.

It is conceivable, nevertheless, that a reduction in $[Mg^{2+}]$ may have contributed to the activation of *phoP* at later times. The limited retention time of PEBBLEs in the vacuoles precluded measurements of $[Mg^{2+}]$ beyond 30 min. Therefore, we used a different approach to assess the possible contribution of reduced $[Mg^{2+}]$ to the activation of *phoP* at longer times. We reasoned that activation of the promoter should be obliterated if any such late reduction in $[Mg^{2+}]$ is pre-

vented. To this end we used divalent cation ionophores to maintain $[Mg^{2+}]$ elevated for up to 2 h. Extracellular Ca^{2+} was omitted in these experiments to avoid the toxicity associated with ionophore-induced elevation of $[Ca^{2+}]$. As documented in Table 1 and Figure 5C, addition of ionophores such as ionomycin or A23187 in the presence of 10 mM MgCl$_2$, induced a marked and sustained elevation of vacuolar $[Mg^{2+}]$, as measured by the PEBBLEs. Having ascertained that $[Mg^{2+}]$ could be clamped at a supraphysiological level, we proceeded to study the induction of PhoP. As shown in Figure 6, the induction of the promoter was unaffected by sustained elevation of vacuolar $[Mg^{2+}]$, indicating that reduction in the concentration of this cation does not
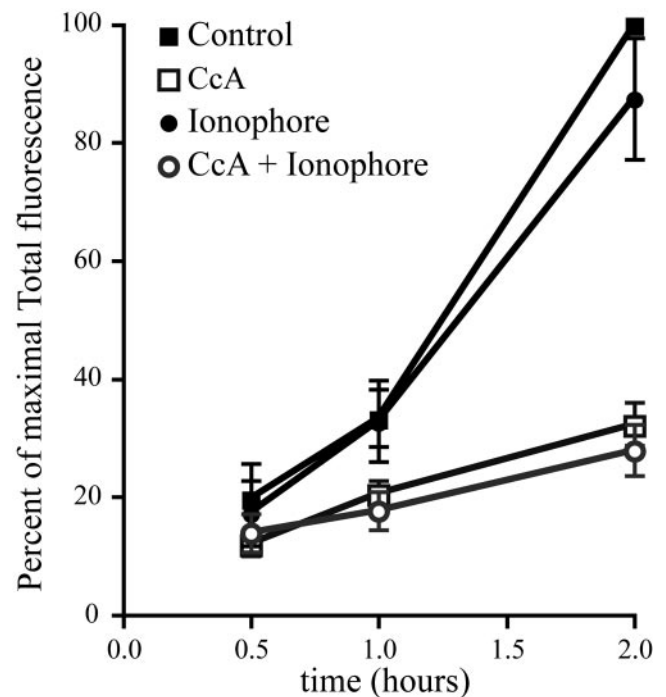

Figure 6. Effect of an imposed elevation of vacuolar $[Mg^{2+}]$ on PhoPQ induction. Intracellular induction of *phoP*::GFP was monitored by flow cytometry in RAW cells infected with *Salmonella* Typhimurium pMLZ205 for 15 min and then otherwise untreated (■), treated with 10 mM MgCl$_2$ plus 4 μM A23187 (●), 30 nM CcA (□), or a combination of CcA, elevated MgCl$_2$ and A23187 (○). The mean total fluorescence $\pm$ SE of at least four different experiments is expressed as percent of the maximal induction of the control for each experiment.
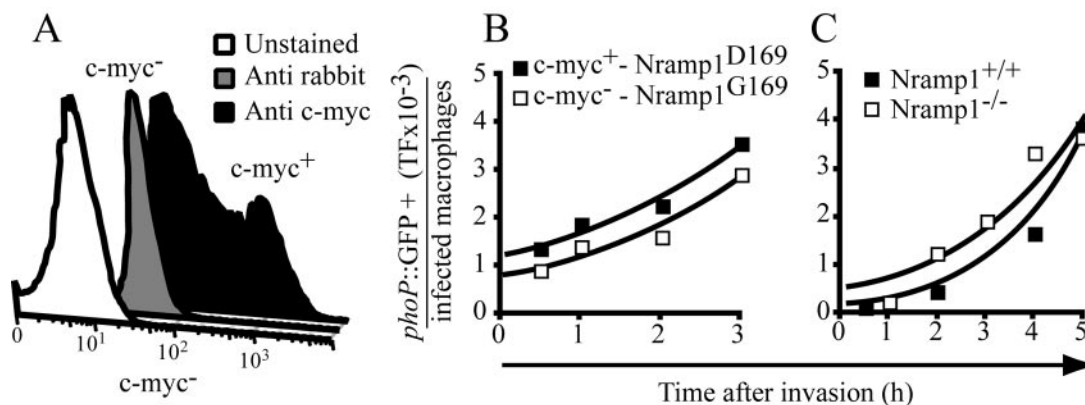
Figure 7. Assessment of the contribution of Nramp1 to the induction of PhoPQ. (A) Identification of cells transfected with Nramp1(G169) by immunostaining of the c-myc epitope tag. Flow cytometric histograms of unstained cells (white), cells stained with the secondary antibody only (gray histogram), and cells with both anti-myc and secondary antibody (black histogram) are shown. (B) RAW264.7 cells expressing Nramp1(G169) or Nramp1(D169) were infected with *Salmonella* Typhimurium pMLZ205 for 15 min using a MOI of 10. Extracellular bacteria were washed and the infected cells incubated for the indicated times. The total green fluorescence (TF) was measured as in Figure 3. (C) Peritoneal macrophages elicited from either Nramp1$^{-/-}$ and Nramp1$^{+/+}$ mice were infected with *Salmonella* Typhimurium transformed with *phoP*::GFP (MOI = 10) as above, and TF was measured cytometrically. Data in A and B are representative of five independent experiments.

play an essential role in *phoP* activation, even at relatively long (2 h) times after infection.

Assessment of the Role of Nramp1 in phoP GFP Induction

We next tested the role of divalent cations other than Mg^{2+} in the induction of PhoPQ. Nramp1, an endomembrane transporter, is thought to extrude divalent cations such as Mn^{2+} and Fe^{2+} from the lumen of phagosomes and bacterial invasion vacuoles, thereby contributing to the microbicidal response (Forbes and Gros, 2003). Nramp1 can transport a variety of inorganic cations, including Fe^{2+} and Mn^{2+} that would not be detected by the PEBBLE system yet may be critical for PhoPQ induction.

To test the role of divalent cation extrusion via Nramp1, we compared cells expressing functional versus inactive transporters. RAW264.7 macrophages bear a homozygous mutant Nramp1 (D169) allele that is not functional and are therefore permissive to the replication of various intracellular parasites, including *Salmonella* Typhimurium. Transfection of an epitope-tagged wild-type Nramp1 (G169) into these cells abrogated intracellular replication of *Salmonella* (Govoni *et al.*, 1999). As shown in Figure 7A, the cells expressing the recombinant protein could be readily identified by flow cytometry. Multicolor cytometric measurements enabled us to analyze the expression of *phoP*::GFP selectively in Nramp1 (G169)-expressing cells, following invasion with *Salmonella* Typhimurium transformed with *phoP*::GFP. As illustrated in Figure 7B, the rate and extent of induction of PhoPQ was similar in cells expressing the functional, wild-type form of Nramp1 and in those with only the mutant, inactive allele. In five determinations, the *phoP*::GFP total fluorescence expression in the mutant cells was equivalent to the one observed in the wild-type Nramp1 transfectants.

A more stringent test of the role of Nramp1 was made using peritoneal macrophages elicited from Nramp1-deficient ($^{-/-}$) and wild-type mice ($^{+/+}$), both on 129Sv background. As found in RAW cells, GFP fluorescence accumulated in the primary murine cells infected with *Salmonella* transformed with *phoP*::GFP (Figure 7C). Consistent with a role of Nramp1 in controlling infection, we found that when analyzed after 5 h the fraction of infected cells was lower in wild-type than in the Nramp1-deficient cells (54% vs. 77%).

When normalized per infected cell, however, the rate of GFP accumulation was indistinguishable in wild-type and null mice (Figure 7C). Taken together, these findings indicate that divalent metal extrusion via Nramp1 is not an important contributor to the induction of PhoP in macrophages. They also imply that Nramp1 controls bacterial infection by mechanisms other than inhibition of PhoPQ induction.

Role of SCV Acidification in the Induction of PhoPQ

We next considered the possible role of luminal pH in the activation of *phoP* promoter inside SCV. To this end we used concanamycin A (CcA), a potent and highly specific inhibitor of the H^+-pumping V-ATPases that are responsible for organellar acidification (Bowman *et al.*, 1988; Yoshimori *et al.*, 1991). We initially confirmed that CcA selectively affects mammalian cells and has no direct effect on the growth of *Salmonella* in vitro. Preliminary experiments were next conducted using acridine orange to define conditions that would obliterate SCV acidification, whether generated by de novo H^+ pumping into the vacuole or by fusion with preacidified organelles of the endocytic pathway (unpublished data). The evolution of GFP fluorescence was monitored by flow cytometry as in the experiments described above. As shown in Figure 8B, induction of *phoP*::GFP in cells pretreated with CcA was markedly diminished (by 72 ± 4% at 2 h and by 90 ± 2% at 3 h; means ± SE of 5 experiments). Detailed analysis of the dot plots as in Figure 3, indicated that two distinct factors contributed to the decrease in the mean fluorescence intensity of the population: 1) the fluorescence accumulated by individual intracellular bacteria was considerably diminished (by 50%) and 2) the ability of the bacteria to invade the macrophages was inhibited by prior dissipation of the cellular pH gradients (see Figure 8D, white triangles). The reduced susceptibility of CcA-pretreated cells to invasion by *Salmonella* was verified independently using cell lysis and bacterial plating (Figure 8E). The mechanism underlying this inhibition of invasion is presently unclear, yet it complicates the interpretation of our results. To obviate the effect of prior dissipation of the pH gradient, a second series of experiments was performed adding CcA only after invasion was completed (see Figure 8A and white squares in 8, B–E). Under these conditions
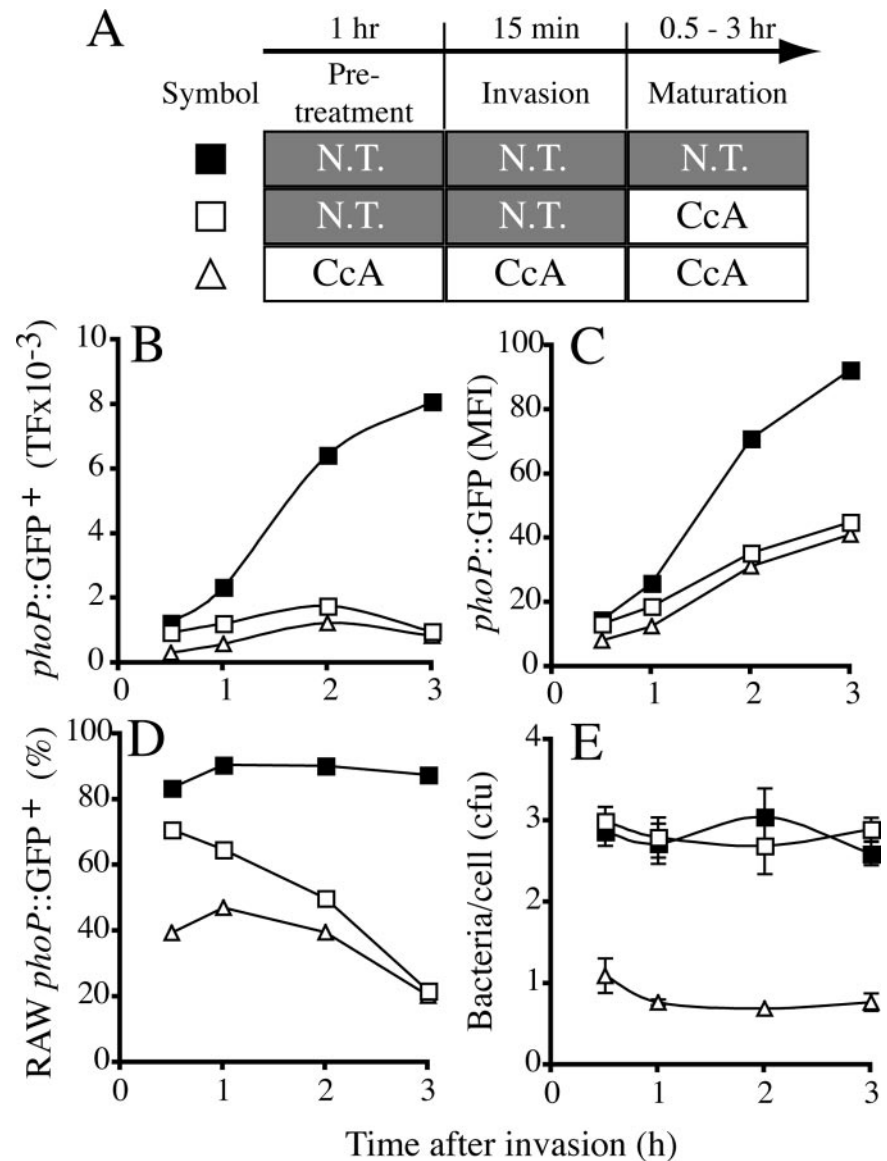
Figure 8. Assessment of the role of vacuolar pH in PhoPQ induction. (A) Experimental design. The diagram indicates when concanamycin A (CcA; 30 nM) was added to the cells with respect to the time of infection. N.T., not-treated with CcA. Note that each protocol corresponds to one of the symbols used in B–E. (B–D) RAW264.7 macrophages subjected to the specific protocol described in A were infected with *Salmonella* Typhimurium pMLZ205 at a MOI of 10 for 15 min and analyzed by flow cytometry at the specified times. (B) Total fluorescence; (C) mean fluorescence intensity of infected cells; (D) percentage of cells expressing GFP. Data in B–D are representative of five similar experiments. (E) Quantitation of viable bacteria recovered from infected cultures, performed by cell lysis and plating of lysates on LB agar plates. Data in E are means ± SE of three independent experiments with triplicates for each determination.

invasion efficiency was unaltered (Figure 8E) and the role of SCV acidification could be studied independently. As shown in Figure 8B, SCV acidification was required for optimal induction of *phoP*::GFP. Only a small fraction of the GFP accumulated in cells that were unable to pump H$^+$. Vacuolar acidification was required to sustain the expression of GFP, because the weak induction observed at early times in CcA-treated cells declined over time (Figure 8, B and D). It is unclear whether the transient initial stimulation was caused by fusion of the SCV with preacidified endomembrane compartments that dissipate their pH gradients slowly upon inhibition of the V-ATPase. However, a small (10–20%) yet significant component of the induction must be attributable to factors other than pH, as it persisted in cells pretreated with CcA (triangles in Figure 8, B–D). We conclude that PhoP induction in the SCV is dependent on two factors: vacuolar acidification, which is responsible for the majority of the activation, plus a pH-independent factor responsible for a smaller fraction of the stimulation. A previous report from Rathman *et al.* (1996) showed that treatment of *Salmonella* Typhimurium-infected RAW cells with bafilomycin (another fungal product that, like CcA, inhibits V-ATPases) induced a gradual reduction in the viability of the intracellular bacteria. Our results contrast with this report in that CcA treatment did not significantly affect survival of *Salmonella* Typhimurium during the first 3 h. The source of this apparent discrepancy is not immediately obvious.

To address whether inhibition of the H$^+$-ATPase and the consequent alkalinization of the vacuole have a direct effect on its [Mg^{2+}], we performed additional measurements using PEBBLEs. The fluorescence ratio of C343 to TxR was not modified when 30 nM of CcA was added to otherwise untreated cells (Table 1). Moreover, the ATPase inhibitor had no effect on the ionophore-imposed elevation of vacuolar [Mg^{2+}] (Table 1). Because CcA depressed PhoP induction in the presence of divalent cation ionophores (Figure 6), without preventing the sustained [Mg^{2+}] elevation, we conclude that the effects of the ATPase inhibitor are mediated directly by changes in pH and not by an indirect alteration of [Mg^{2+}] homeostasis.
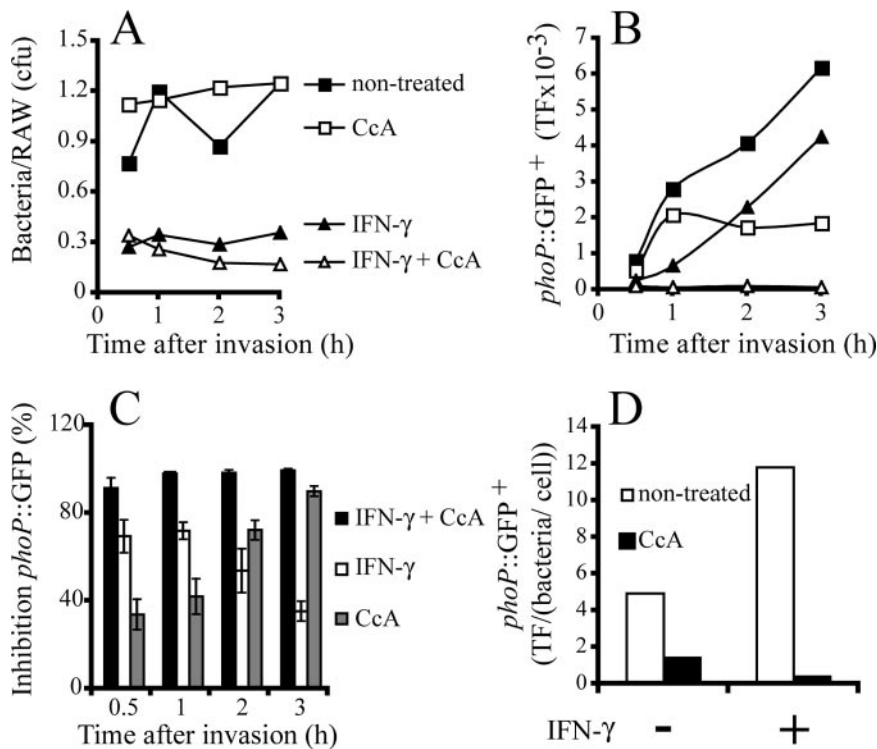
Figure 9. Effect of pretreatment with IFNγ on PhoPQ induction. RAW264.7 macrophages were either pretreated for 18 h with 100 U of IFNγ (triangles) or were left untreated (squares). The cells were infected with *Salmonella* Typhimurium transformed with *phoP*::GFP and analyzed by flow cytometry as above. Where indicated, the cells were in addition treated with CcA immediately after invasion (as for the open squares in Figures 7 and 8). (A) Quantitation of viable bacteria recovered from infected cultures, performed by cell lysis and plating of lysates on LB agar plates; (B) total fluorescence. (C) Percentage of inhibition of *phoP*::GFP expression by IFN-γ, CcA and the combination of both IFN-γ and CcA. (D) Fluorescence normalized per bacterium, per cell. Data shown in A, B, and D are representative of five similar experiments and C is a compilation of five independent experiments.

To test whether the induction of PhoP was measurable also in nonphagocytic cells, we infected HeLa and MDCK cells with *Salmonella* Typhimurium pMLZ205 and followed GFP expression by flow cytometry. The induction of PhoP was clearly detectable within these two epithelioid cell lines, although with somewhat different kinetics (Supplementary Figure 3A). As found earlier for RAW264.7 cells, the induction was highly sensitive to treatment of the cells with CcA (Supplementary Figure 3B). These results suggest that the induction of the PhoP-controlled genes in bacteria that enter epithelial cells is regulated primarily by the acidification of the SCV, as it is in macrophages.

IFNγ Reduces Invasion Efficiency but Promotes PhoP Induction

The preceding results point to the existence of one or more factors, distinct from changes in pH and [Mg^{2+}], that contribute to the early expression of PhoPQ by intracellular *Salmonella*. We therefore tested the effects of IFNγ, a potent cytokine that increases the bactericidal functions of macrophages by a variety of mechanisms, including stimulation of protease production, induction of nitric oxide-synthase (iNOS) and of components of the NADPH oxidase, and activation of endocytosis (Boehm *et al.*, 1997). RAW264.7 macrophages were pretreated with 100 U of IFNγ for 18 h before bacterial invasion. As expected from its reported microbicidal effects, treatment with IFNγ greatly reduced the number of viable bacteria found inside macrophages 3 h after infection (Figure 9A). Analysis of the kinetics of the process indicated, however, that the reduced bacterial count was a consequence of reduced invasion, because the number of internal bacteria was curtailed by IFNγ from the earliest time tested (30 min) and did not decrease significantly for the following 2.5 h. Consistent with the reduced invasion, the total GFP fluorescence of the infected population was lower after 30 min and remained depressed for an additional

30 min (Figure 9B). Remarkably, in the IFNγ-treated cells GFP accumulation progressed very rapidly thereafter (Figure 9B). When calculated per intracellular bacterium, the induction of *phoP*::GFP measured after 3 h was considerably greater in IFNγ-treated than in control cells (Figure 9D).

In THP-1 monocytes, IFNγ treatment was found to modify the luminal pH of vacuoles containing *Coxiella* (Ghigo *et al.*, 2002). It was therefore conceivable that the effect of IFNγ on *phoP*::GFP induction was caused by an accentuated acidification. We therefore tested the role of V-ATPases in the stimulatory effect of IFNγ. When tested in combination, CcA and IFNγ virtually eliminated the induction of *phoP*::GFP (Figure 9B, triangles, and 9C). This observation implies that stimulation of PhoP expression by IFNγ requires V-ATPase activity and may result from a more profound SCV acidification.

To test the latter notion directly, we measured the luminal pH of SCV formed in control and IFNγ-pretreated cells. To this end, *Salmonella* were covalently labeled with a pH-sensitive fluorescent dye. After invasion by the labeled bacteria, the fluorescence emission of the probe was analyzed by digital imaging using two excitation wavelengths. The absolute pH was deduced from the fluorescence ratio, using in situ calibration (see *Materials and Methods*). In six determinations, the pH of the SCV ranged between 6.5 and 5.8 in cells that had not been treated with IFNγ (mean = 6.38 ± 0.29). The vacuolar pH of cells pretreated with IFNγ was not different (6.3 ± 0.27). We concluded that stimulation of PhoPQ induction by the cytokine required SCV acidification, but was not directly attributable to differences in vacuolar pH.

DISCUSSION

Garcia-del Portillo *et al.* (1992) detected induction of mgtB, a PhoPQ-controlled gene in bacteria within SCV, and inter-

preted the data to mean [Mg^{2+}] was low inside the vacuole. This premise is based on the marked effects exerted by this cation on PhoPQ induction in vitro (Soncini *et al.,* 1996 and see also Figure 1) and rests on the assumption that [Mg^{2+}] is also the predominant, if not the sole determinant of PhoPQ in vivo (Garcia Vescovi *et al.,* 1996; Groisman, 2001; Soncini *et al.,* 1996). Contrary to this notion, we found that changes in [Mg^{2+}] play a comparatively minor role in the early expression of PhoP within the SCV, at least in macrophages. This conclusion is based on the following findings: 1) *phoP* induction is apparent within the first 30 min of invasion and direct measurements of [Mg^{2+}] failed to detect a significant drop during this period of time; 2) attempts to manipulate the [Mg^{2+}] of the SCV failed to modify the sustained expression of *phoP*::GFP, and 3) induction was attributable to luminal acidification. We verified that alteration in pH did not impair [Mg^{2+}] homeostasis nor our ability to artificially clamp [Mg^{2+}] using ionophores. The observation that acidification itself suffices to induce PhoP makes control of the *phoP* promoter by the pH of the SCV the preferred hypothesis.

Extrusion from the vacuole of divalent cations other than Mg^{2+} is similarly unlikely to be a critical determinant of PhoP induction, because elimination or ectopic expression of Nramp1 in macrophages had no significant effect on the expression of GFP in SCVs formed in primary macrophages or in transfected macrophage cell lines. Moreover, Nramp1 is expressed only in myeloid cells and not in epithelia, where PhoP was also activated. Nramp1 is a pH-dependent divalent cations efflux pump at the phagosomal membrane, which is thought to act by restricting the luminal availability of different metals that may be required for intracellular replication of bacteria, including *Salmonella*. Recently, Zaharik *et al.* (2004) observed in RAW264.7 macrophages that Nramp1-mediated metal depletion causes increased expression of the Mn^{2+}/Fe^{2+} transporters MntH and SitA, consistent with the idea that Nramp1-positive SCVs are depleted for these metals. These findings, together with the lack of effect of Nramp1 on PhoPQ induction noted in the present study, indicate that: 1) Mn and Fe do not play an important role in induction of PhoPQ in SCVs, and 2) the bacteriostatic/bactericidal mechanism of Nramp1 action is independent of modulation of PhoPQ. Our findings are also consistent with previous results (Cuellar-Mata *et al.,* 2002) showing that SCVs formed in Nramp1-positive and Nramp1-negative macrophages acidify to the same extent, accounting for the comparable levels of PhoP induction.

Alpuche-Aranda *et al.* (1992) demonstrated that dissipation of the pH gradient across the SCV depressed the induction of PhoPQ, identifying luminal acidification as an important in situ determinant of induction. This notion was confirmed and further examined in our manuscript, where the kinetics of the events and the relative contribution of pH and other factors on PhoPQ activation were further clarified. The major role of pH in PhoPQ induction could be direct, by protonation of one or more bacterial components that control gene expression. However, the effect may be indirect, perhaps by competitively dislodging Mg^{2+} from its binding sites on PhoQ. Alternatively, acidification may control fusion of the SCV with endomembrane compartments that may deliver oxidants, peptides, proteases, or other potential activators of PhoPQ. In fact, it was recently demonstrated that cationic antimicrobial peptides are potent inducers of PhoPQ (Bader *et al.,* 2005) and can regulate *Salmonella* replication in macrophages (Rosenberger *et al.,* 2004). The widely disparate nature of PhoPQ agonists suggests that the complex may in fact be a sensor of membrane shape and/or

rigidity. The well established role of Mg^{2+} in the maintenance of the bacterial wall structure (Guo *et al.,* 1998) would explain its effects on induction, whereas the addition of cationic peptides may cluster negatively charged moieties on the bacterial wall, resulting in its deformation. Protonation of components of the wall or membrane could have a similar effect. As well, protons may affect PhoQ by participating in the binding or generation of cationic peptides from their precursors. Finally, a PhoQ-independent mechanism of activation of PhoP target genes was recently demonstrated (Lejona *et al.,* 2004), which may also be controlled by vacuolar acidification.

We also detected a CcA-resistant, presumably acidification-independent component of the induction, though its underlying mechanism remains undefined. Interestingly, this secondary component was eliminated when the cells were pretreated with IFNγ, despite the fact that IFNγ per se was a net activator of PhoPQ induction. Multiple processes are activated by IFNγ pretreatment and some of these could potentiate PhoPQ expression. In addition, enhanced secretion of proteases, antimicrobial peptides or reactive oxygen species may contribute to membrane destabilization and activation of PhoPQ. Some of these events may act synergistically with vacuolar acidification. Thus, lysosomal proteases have acidic pH optima and the dismutation of superoxide requires protons. In this manner, the PhoPQ system appears to be ideally poised to sense the adverse conditions developing within the SCV and is thereby capable of alerting and preparing the bacterium for intracellular survival.

REFERENCES

Alpuche Aranda, C. M., Swanson, J. A., Loomis, W. P., and Miller, S. I. (1992). *Salmonella typhimurium* activates virulence gene transcription within acidified macrophage phagosomes. Proc. Natl. Acad. Sci. USA *89*, 10079–10083.

Amer, A. O., and Swanson, M. S. (2002). A phagosome of one's own: a microbial guide to life in the macrophage. Curr. Opin. Microbiol. *5*, 56–61.

Bader, M. W., Navarre, W. W., Shiau, W., Nikaido, H., Frye, J. G., McClelland, M., Fang, F. C., and Miller, S. I. (2003). Regulation of *Salmonella typhimurium* virulence gene expression by cationic antimicrobial peptides. Mol. Microbiol. *50*, 219–230.

Bader, M. W., Sanowar, S., Daley, M. E., Schneider, A. R., Cho, U., Xu, W., Klevit, R. E., Le Moual, H., and Miller, S. I. (2005). Recognition of antimicrobial peptides by a bacterial sensor kinase. Cell *122*, 461–472.

Bearson, B. L., Wilson, L., and Foster, J. W. (1998). A low pH-inducible, PhoPQ-dependent acid tolerance response protects *Salmonella typhimurium* against inorganic acid stress. J. Bacteriol. *180*, 2409–2417.

Boehm, U., Klamp, T., Groot, M., and Howard, J. C. (1997). Cellular responses to interferon-gamma. Annu. Rev. Immunol. *15*, 749–795.

Bowman, E. J., Siebers, A., and Altendorf, K. (1988). Bafilomycins: a class of inhibitors of membrane ATPases from microorganisms, animal cells, and plant cells. Proc. Natl. Acad. Sci. USA *85*, 7972–7976.

Clark, H. A., Hoyer, M., Philbert, M. A., and Kopelman, R. (1999). Optical nanosensors for chemical analysis inside single living cells. 1. Fabrication, characterization, and methods for intracellular delivery of PEBBLE sensors. Anal. Chem. *71*, 4831–4836.

Cuellar-Mata, P., Jabado, N., Liu, J., Furuya, W., Finlay, B. B., Gros, P., and Grinstein, S. (2002). Nramp1 modifies the fusion of *Salmonella typhimurium*-containing vacuoles with cellular endomembranes in macrophages. J. Biol. Chem. *277*, 2258–2265.

Forbes, J. R., and Gros, P. (2003). Iron, manganese, and cobalt transport by Nramp1 (Slc11a1) and Nramp2 (Slc11a2) expressed at the plasma membrane. Blood *102*, 1884–1892.

Garcia Vescovi, E., Soncini, F. C., and Groisman, E. A. (1996). Mg2+ as an extracellular signal: environmental regulation of *Salmonella* virulence. Cell *84*, 165–174.

Garcia-del Portillo, F., Foster, J. W., Maguire, M. E., and Finlay, B. B. (1992). Characterization of the micro-environment of *Salmonella typhimurium*-containing vacuoles within MDCK epithelial cells. Mol. Microbiol. *6*, 3289–3297.

Garvis, S. G., Beuzon, C. R., and Holden, D. W. (2001). A role for the PhoP/Q regulon in inhibition of fusion between lysosomes and *Salmonella*-containing vacuoles in macrophages. Cell Microbiol. *3*, 731–744.

Ghigo, E., Capo, C., Tung, C. H., Raoult, D., Gorvel, J. P., and Mege, J. L. (2002). *Coxiella* burnetii survival in THP-1 monocytes involves the impairment of phagosome maturation: IFN-gamma mediates its restoration and bacterial killing. J. Immunol. *169*, 4488–4495.

Govoni, G., Canonne-Hergaux, F., Pfeifer, C. G., Marcus, S. L., Mills, S. D., Hackam, D. J., Grinstein, S., Malo, D., Finlay, B. B., and Gros, P. (1999). Functional expression of Nramp1 in vitro in the murine macrophage line RAW264.7. Infect. Immun. *67*, 2225–2232.

Groisman, E. A. (2001). The pleiotropic two-component regulatory system PhoP-PhoQ. J. Bacteriol. *183*, 1835–1842.

Groisman, E. A., Kayser, J., and Soncini, F. C. (1997). Regulation of polymyxin resistance and adaptation to low-Mg2+ environments. J. Bacteriol. *179*, 7040–7045.

Guina, T., Yi, E. C., Wang, H., Hackett, M., and Miller, S. I. (2000). A PhoP-regulated outer membrane protease of *Salmonella enterica* serovar typhimurium promotes resistance to alpha-helical antimicrobial peptides. J. Bacteriol. *182*, 4077–4086.

Guo, L., Lim, K. B., Gunn, J. S., Bainbridge, B., Darveau, R. P., Hackett, M., and Miller, S. I. (1997). Regulation of lipid A modifications by *Salmonella typhimurium* virulence genes phoP-phoQ. Science *276*, 250–253.

Guo, L., Lim, K. B., Poduje, C. M., Daniel, M., Gunn, J. S., Hackett, M., and Miller, S. I. (1998). Lipid A acylation and bacterial resistance against vertebrate antimicrobial peptides. Cell *95*, 189–198.

House, D., Bishop, A., Parry, C., Dougan, G., and Wain, J. (2001). Typhoid fever: pathogenesis and disease. Curr. Opin. Infect. Dis. *14*, 573–578.

Jabado, N., Tseung-Yuk-Lam, S., Forbes, J. R., and Gros, P. (2004). Mouse natural resistance associated macrophage protein 1 (Nramp1): a key regulator of host innate immunity against infections. In: The Nramp Family, ed. Cellier, M., and Gros, P., New York: Kluwer Academic/Plenum Publishers, 1–15.

Lejona, S., Castelli, M. E., Cabeza, M. L., Kenney, L. J., Garcia Vescovi, E., and Soncini, F. C. (2004). PhoP can activate its target genes in a PhoQ-independent manner. J Bacteriol. *186*, 2476–2480.

Mastroeni, P., Harrison, J. A., Robinson, J. H., Clare, S., Khan, S., Maskell, D. J., Dougan, G., and Hormaeche, C. E. (1998). Interleukin-12 is required for control of the growth of attenuated aromatic-compound-dependent salmonellae in BALB/c mice: role of gamma interferon and macrophage activation. Infect. Immun. *66*, 4767–4776.

Miller, S. I., Kukral, A. M., and Mekalanos, J. J. (1989). A two-component regulatory system (phoP phoQ) controls *Salmonella typhimurium* virulence. Proc. Natl. Acad. Sci. USA *86*, 5054–5058.

Mirza, S. H., Beeching, N. J., and Hart, C. A. (1996). Multi-drug resistant typhoid: a global problem. J. Med. Microbiol. *44*, 317–319.

Monack, D. M., Bouley, D. M., and Falkow, S. (2004). *Salmonella typhimurium* persists within macrophages in the mesenteric lymph nodes of chronically

infected Nramp1+/+ mice and can be reactivated by IFNγ neutralization. J. Exp. Med. *199*, 231–241.

Nauciel, C., and Espinasse-Maes, F. (1992). Role of gamma interferon and tumor necrosis factor alpha in resistance to *Salmonella typhimurium* infection. Infect. Immun. *60*, 450–454.

Park, E. J., Brasuel, M., Behrend, C., Philbert, M. A., and Kopelman, R. (2003). Ratiometric optical PEBBLE nanosensors for real-time magnesium ion concentrations inside viable cells. Anal. Chem. *75*, 3784–3791.

Pie, S., Truffa-Bachi, P., Pla, M., and Nauciel, C. (1997). Th1 response in *Salmonella typhimurium*-infected mice with a high or low rate of bacterial clearance. Infect. Immun. *65*, 4509–4514.

Rathman, M., Sjaastad, M. D., and Falkow, S. (1996). Acidification of phagosomes containing *Salmonella typhimurium* in murine macrophages. Infect. Immun. *64*, 2765–2773.

Rosenberger, C. M., Gallo, R. L., and Finlay, B. B. (2004). Interplay between antibacterial effectors: a macrophage antimicrobial peptide impairs intracellular *Salmonella* replication. Proc. Natl. Acad. Sci. USA *101*, 2422–2427.

Shea, J. E., Hensel, M., Gleeson, C., and Holden, D. W. (1996). Identification of a virulence locus encoding a second type III secretion system in *Salmonella typhimurium*. Proc. Natl. Acad. Sci. USA *93*, 2593–2597.

Soncini, F. C., Garcia Vescovi, E., Solomon, F., and Groisman, E. A. (1996). Molecular basis of the magnesium deprivation response in *Salmonella typhimurium*: identification of PhoP-regulated genes. J. Bacteriol. *178*, 5092–5099.

Soncini, F. C., Vescovi, E. G., and Groisman, E. A. (1995). Transcriptional autoregulation of the *Salmonella typhimurium* phoPQ operon. J. Bacteriol. *177*, 4364–4371.

Vazquez-Torres, A., Jones-Carson, J., Baumler, A. J., Falkow, S., Valdivia, R., Brown, W., Le, M., Berggren, R., Parks, W. T., and Fang, F. C. (1999). Extraintestinal dissemination of *Salmonella* by CD18-expressing phagocytes. Nature *401*, 804–808.

Vazquez-Torres, A., Jones-Carson, J., Mastroeni, P., Ischiropoulos, H., and Fang, F. C. (2000). Antimicrobial actions of the NADPH phagocyte oxidase and inducible nitric oxide synthase in experimental salmonellosis. I. Effects on microbial killing by activated peritoneal macrophages in vitro. J. Exp. Med. *192*, 227–236.

Wick, M. J. (2004). Living in the danger zone: innate immunity to *Salmonella*. Curr. Opin. Microbiol. *7*, 51–57.

Yoshimori, T., Yamamoto, A., Moriyama, Y., Futai, M., and Tashiro, Y. (1991). Bafilomycin A1, a specific inhibitor of vacuolar-type H(+)-ATPase, inhibits acidification and protein degradation in lysosomes of cultured cells. J. Biol. Chem. *266*, 17707–17712.

Young, D., Hussell, T., and Dougan, G. (2002). Chronic bacterial infections: living with unwanted guests. Nat. Immunol. *3*, 1026–1032.

Zaharik, M. L., Cullen, V. L., Fung, A. M., Libby, S. J., Kujat Choy, S. L., Coburn, B., Kehres, D. G., Maguire, M. E., Fang, F. C., and Finlay, B. B. (2004). The *Salmonella enterica* serovar typhimurium divalent cation transport systems MntH and SitABCD are essential for virulence in an Nramp1G169 murine typhoid model. Infect. Immun. *72*, 5522–5525.